

A low-cost IoT-based deep learning method of water gauge measurement for flood monitoring

Leila Hashemi-Beni, Megha Puthenparampil & Ali Jamali

To cite this article: Leila Hashemi-Beni, Megha Puthenparampil & Ali Jamali (2024) A low-cost IoT-based deep learning method of water gauge measurement for flood monitoring, *Geomatics, Natural Hazards and Risk*, 15:1, 2364777, DOI: [10.1080/19475705.2024.2364777](https://doi.org/10.1080/19475705.2024.2364777)

To link to this article: <https://doi.org/10.1080/19475705.2024.2364777>



© 2024 The Author(s). Published by Informa UK Limited, trading as Taylor & Francis Group.



Published online: 08 Jul 2024.



Submit your article to this journal [↗](#)



Article views: 2085



View related articles [↗](#)



View Crossmark data [↗](#)



A low-cost IoT-based deep learning method of water gauge measurement for flood monitoring

Leila Hashemi-Beni^a, Megha Puthenparampil^a and Ali Jamali^b

^aDepartment of Built Environment, College of Science and Technology, NC A&T State University, Greensboro, NC, USA; ^bDepartment of Geography, Simon Fraser University, Burnaby, Canada

ABSTRACT

Real-time and accurate measurement of the water level is a critical step in flood monitoring and management of water resources. In recent years, with the advent of the Internet of Things (IoT) and cloud computing platforms and resources, the surveillance technology for water monitoring has been revolutionized due to the availability of high-resolution and portable cameras, robust image processing techniques, and cloud-enabled data fusion centers. However, despite the potential advantages of online water level monitoring of the rivers and lakes, some technical challenges need to be addressed before they can be fully utilized. Submersible sensor devices are frequently used for measuring water levels but are prone to damage from sediment deposition and many gauge detection techniques are inefficient at nighttime. In response, this paper presents a novel Internet of Things (IoT) based deep learning methodology that uses Mask-RCNN to accurately segment gauges from images even when there are distortions present. An automated and immediate water stage estimate is provided by this simple, low-cost method. The methodology's applicability to water resource management systems and flood disaster prevention engineering opens up new possibilities for the deployment of intelligent IoT-based flood monitoring systems in the future.

ARTICLE HISTORY


Received 22 October 2023
Accepted 1 June 2024

KEYWORDS

Water level measurement;
remote sensing; image
processing; deep learning;
low-cost surveillance system

1. Introduction

The use of cameras, sensors, and internet connectivity in remote sensing technologies is expanding and becoming increasingly accessible for monitoring and preserving public safety in a variety of contexts. Climate change, in the context of global warming, has resulted in unusual weather events like powerful storms and flooding, the forecasting of which depends on remote monitoring capabilities. The worldwide frequency of hurricanes and thunderstorms with significant precipitation has been attributed to a gradual increase in global temperatures (Smith and Katz 2013). Periodically, intense, locally

CONTACT Leila Hashemi-Beni  lhashemibeni@ncat.edu

© 2024 The Author(s). Published by Informa UK Limited, trading as Taylor & Francis Group.

This is an Open Access article distributed under the terms of the Creative Commons Attribution License (<http://creativecommons.org/licenses/by/4.0/>), which permits unrestricted use, distribution, and reproduction in any medium, provided the original work is properly cited. The terms on which this article has been published allow the posting of the Accepted Manuscript in a repository by the author(s) or with their consent.

concentrated downpours may result in flash flooding, particularly in rural areas lacking adequate infrastructure and in floodplains (Villarini 2016). Both rural and urban areas are more susceptible to flooding. As a result, disaster risk assessment and flood prediction in locations close to waterways depend heavily on real-time monitoring. Different systems for measuring flood levels and water levels have been developed in response to these challenges. Conventional flood monitoring mainly depends on physical gauge stations, but they are expensive and have a limited coverage area. While real-time capability is lacking, recent advancements in satellite-based remote sensing offer greater visibility. However, there are a few potential cons of using satellite imagery for flood monitoring, such as heavy cloud cover obstructing the view, areas covered by vegetation (Salem and Hashemi-Beni 2022), and interpreting satellite images requires complex analysis. There have been various studies on various cloud removal in satellite images recently, but it still needs further exploration (Ling et al. 2021).

The use of ground-based camera networks for real-time flood monitoring has been investigated recently as cameras become more affordable and prevalent in urban areas (Jafari et al. 2020; Sood et al. 2018). Consumer or commercial cameras can detect minute variations in water level that are essential for calibration, they even have physical resolution down to millimeters. Ground cameras cover a larger area than individual sensors and offer localized visibility that satellites cannot. Video streams from custom installations and closed-circuit television (CCTV) infrastructure have both been studied. CCTV mounted on the ground or specially designed cameras provide localized, weather- and cloud-independent real-time visual feeds. In particular, fixed video streams can recognize flooded areas in the camera's field of view by using the boundaries of the water. Without the need for object recognition models, computer vision techniques such as background subtraction (Basnyat et al. 2018) make it possible to detect objects in the foreground, such as flooded zones. On the other hand, obstacles include occlusion, visibility restrictions, and environmental factors. However, research on developing robust perception algorithms is still ongoing in contrast to operational reliability. Still camera networks provide critical visibility that sensors alone cannot, particularly across urban waterways or flood-protection infrastructure (Pan et al. 2018). Ground-based camera networks combined with computer vision techniques have the potential for real-time flood detection. However, extensive manual analysis is still required in most cases. Other gauge sensor techniques, such as float transmitters, require the installation of significant infrastructure at fixed sites along the body of water. Equipment must be physically connected by transmission lines, which reduces site flexibility. However, wireless cameras that run on batteries can be deployed more quickly. Beyond point measurements from gauge sensors, the assimilation of flood models also benefits from localized visual data on the water state (Annis et al. 2019). That being said, aerial or satellite platforms offer a wider field of view for general flood mapping that ground cameras cannot match. However, ground CCTV and stations provide unparalleled benefits for enabling real-time flood prediction through the assimilation of high-resolution gauge data, which is necessary for calibrating models. Currently, no other airborne or spaceborne remote sensing technology can match their ability to physically resolve fine water dynamics in a bounded localized area.

Deep learning models like Convolutional neural networks (CNNs), have already demonstrated early promise in automating the analysis of such visual data to determine areas that have flooded, map the extent of floods, and estimate the flow or depth of water (Gebrehiwot et al., 2019; Gebrehiwot and Hashemi-Beni 2020). Specifically, supervised deep convolutional neural networks (CNNs) like the U-Net method can converge to the edge of the water body faster and more precisely (Xu et al. 2024). For example, Suh et al. employ the weighted Mask R-CNN for improving adjacent boundary segmentation (Suh et al. 2021). Flood regions and boundaries can be defined by simultaneously detecting objects and segmenting instances using architectures such as Mask R-CNN. A combination of CNN and Long-Short Term Memory (LSTM) was used in the study by Baek et al. for water level prediction and monitoring (Baek et al. 2020). GANs are also explored in areas of water level extraction studies, for example, Chen et al. used surveillance images and deployed a CA-GAN model for water level reading (Han et al. 2022). On the sensor side, battery-powered wireless nodes such as rainfall meters and water-level gauges are coordinated by the Internet of Things (IoT). With real-time, affordable, and scalable sensor grids, the IoTs present a great promise for resolving enduring challenges with real-time monitoring, and low-cost scalable sensor grids. Recent IoT research has employed water level sensors for inexpensive monitoring. IoT system with an ultrasonic sensor for flood warning and monitoring is explored in many studies (Rahayu et al. 2023), and liquid volume monitoring based on an ultrasonic sensor and Arduino was developed by Husni et al. (2016). However, these approaches have problems with sensor calibration, the low range of these sensors and ultrasonic sensors are prone to sound and temperature interference. Using real-world IoT sensor data streams, end-to-end deep learning may make it possible to monitor floods automatically and robustly around the clock. This strategy could offer reliable, low-cost alertness for early flood warning and emergency preparedness. IoT-based water level monitoring offers encouraging possibilities, but measurement precision and consistency issues still exist. When applied to large amounts of real-world IoT data, deep learning techniques may be able to overcome these difficulties. For instance, the study by Arshad et al. 2019 explored flood monitoring by using both IT and computer vision and provides a systematic review of flood monitoring in coastal areas. An LSTM-based approach for forecasting water quality in IoT Systems was proposed by Thai-Nghe et al. (2020). CNN coupled with IoT was studied for automated water reading by Li et al. (2019). These studies indicate that, when compared to simple IoT implementations that rely solely on traditional computer vision or control algorithms, deep learning models can improve the accuracy, reliability, insights, and efficiency of IoT-based water level monitoring systems. Combining deep learning with IoT sensing offers several benefits, such as learning from multi-modal heterogeneous data, generalizing to various environments, compensating for errors and noise in the sensors, and enhancing the adaptive and autonomous capabilities of the systems. For big sensor networks, deep learning is also more scalable. Using deep learning for intelligent data analysis and IoT for low-cost sensing and connectivity, this combined approach makes the most of both technologies.

A lot of times, severe flooding happens at night or in severe conditions when visibility is poor. However, daytime visibility is still the main focus of most research at this time. For full flood monitoring resilience, expanding to low-contrast and nighttime environments continues to be an innovation requirement. Data augmentation techniques can produce more artificial training data during the night to further improve the robustness of the model. This lessens reliance on challenging late-night data collection. Nonetheless, consistent round-the-clock surveillance of increasing water levels via ground-based cameras is still an unresolved issue that has received less attention thus far in contrast to instances during the day. The majority of research currently concentrates on visibility during the day. For full flood monitoring resilience, expanding to low-contrast and nighttime environments is still a necessary innovation. When details are obscured, current spectrum techniques are unable to analyze imagery effectively for flood gauging or localization in low light. Research into reliable models that can withstand challenging lighting conditions is therefore necessary for automated gauge reading. To solve the issue of accurate low-light water level estimation from ground cameras, this paper looks into various approaches. In particular, we devise a method that makes use of both traditional computer vision and deep learning methods for gauge reading, and IOT to enable real-time flood monitoring. To address the aforementioned issues, our research develops a low-cost, real-time water level monitoring system that tracks water levels during the day, dawn, dusk, and low light conditions.

Currently, many places lack flood gauges to keep track of water levels. Current gauges also need a substantial, costly infrastructure. This means that gauges used to warn about flooding are inaccessible to small towns and developing areas. This problem might be resolved by new technologies like deep learning algorithms and inexpensive IoT sensors. IoT sensors are small, internet-connected gadgets that can monitor rainfall, water level, and other variables, far less expensive than big, intricate gauges. Meanwhile, deep learning analyzes sensor data and camera images automatically using artificial intelligence to predict the risk of flooding (Gebrehiwot and Hashemi-Beni 2020; Hashemi-Beni and Gebrehiwot 2021). This makes monitoring automatic. IoT sensors that are simple to install in combination with this duo can expand the gauges' reach. Even when certain sensors malfunction, deep learning combines measurements to provide precise and helpful alerts. Although this technological pair is still young, they have the potential to provide accessible flood monitoring wherever it is needed. Expansion of real-world deployments is still being researched. This makes our approach novel and cost-effective. The novelty of this method stems from its practical and engineering solution to address a challenging issue in the field of remote sensing. The aim is to provide life-saving gauge systems to small towns. Flood risk is increasing due to climate change, novel and accessible techniques for threat monitoring could save lives. IoT and deep learning when combined, provide global benchmarks for addressing growing climate-related risks.

Moreover, in literature, there are some customary assumptions about testing images. In particular, it is often assumed that the shooting angle is approximately orthographic, and the camera positions remain constant. However, these ideal conditions are rarely met in practical scenarios due to the limitations imposed by

environmental factors, such as wind. However, we have introduced a tilt correction mechanism to address this issue. The main challenges we explore in this image-based water level measurement are (1) the poor visibility due to non-satisfactory ambient light and various image distortions such as image tilt, (2) the effect of noises (3) and effective real-time water level monitoring. We have developed a computationally efficient mechanism for online monitoring of the water level using both image processing approaches and deep learning methods. The general idea of developing such methods was initially motivated by the North Carolina Emergency Management (NCEM) which required a fast and reliable method for online monitoring of the water level in rivers and lakes in North Carolina. The rest of this paper is organized as follows. [Section 2](#) consists of the details of the measurement site and the equipment used in this study. [Section 3](#) describes the proposed water level measurement methodology integrated with a series of image segmentation algorithms. In [Section 3](#) after image preprocessing and RGB to grayscale conversion, we investigate two methods for image segmentation, including traditional image processing and a deep learning method. In addition, we developed and analyzed two different methods for reading the water gauge. [Section 4](#) discusses and analyzes the results and the importance of the proposed methods from an IoT point of view and suggests research directions to improve on the existing results. [Section 5](#) concludes the paper and provides a summary of the research findings.

2. Measurement site and system

The measurement site is located at the North Carolina Agriculture and Technical State University (NC A&T) farm, in Greensboro, North Carolina. [Figure 1](#) presents our test bed for accumulating data. This is a practical installation of the camera and staff gauge by the NCEM. The sensing system consists of a 2019 Blackhawk LTE Covert Scouting Camera with a picture resolution of 20 MP, video resolution of 1080 P, 720 P, WVGA, and equipped with a multi-zone PIR sensor. The camera's field



Figure 1. The test bed for data accumulation, including a staff gauge and the utilized camera.

of view (FOV) is 58 degrees horizontal and 32 degrees vertical. The latest LTE technology has improved battery life and the speed of wireless functions. The gauge used is Evigia Fiberglass Stream Gauge, 0–4 Feet, graduated in feet/10ths/100ths. The stream gauge is constructed of rugged fiberglass that will not rust, rot, or corrode. The staff gauges are commonly used in practical applications for monitoring the water level in rivers and lakes. Note that these gauges are usually mounted on the rivers' bank or the side of the lakes for stability during floods. As shown in [Figure 1](#), the staff gauge is not placed in the middle of the lake/river; rather it is installed near the land. The images provided by the sensing system are used for the development of image segmentation algorithms and accuracy assessment.

3. Methodology

The overall architecture of the proposed methodology is presented in [Figure 2](#). With the recent advancements in imaging technology, the applications of image identification are increasing in various fields of remote sensing. In this research, we implement

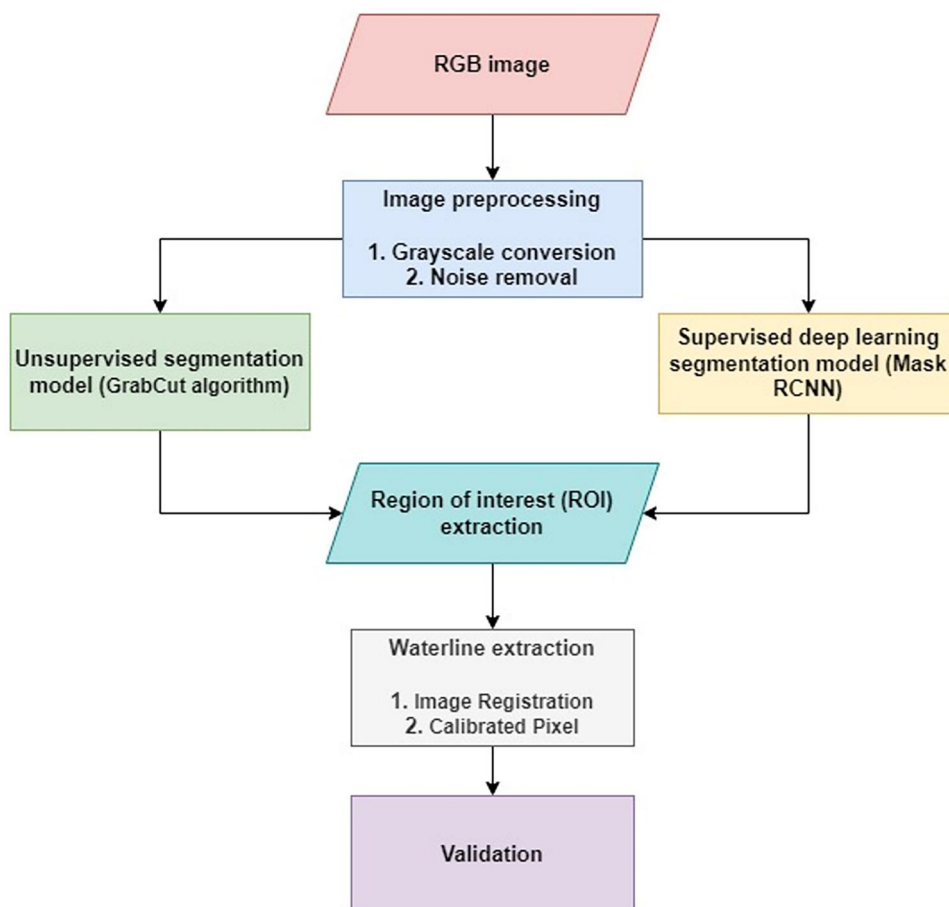


Figure 2. Overall architecture design of the proposed IoT-based water gauge measurement for flood monitoring.

and compare two well-known image identification techniques to measure water levels in rivers and lakes to extract vital information for flood monitoring and disaster management. The details of the proposed techniques are outlined in this section.

3.1. Preprocessing

In this study, preprocessing methods were used on the collected image data to improve algorithmic performance, feature extraction, and computational efficiency. To maximize the input data for the supervised and unsupervised segmentation methods, two essential preprocessing steps—grayscale conversion and noise removal—were methodically used. The first step was to convert color images to grayscale, which lowered the dimensionality of the data. The processed data was then further refined by noise removal which helps algorithms be more robust, accurate, and reliable overall. This is especially true for tasks like object detection, image segmentation, image registration, and pixel calibration. It contributes to ensuring that information in the input images that is false or irrelevant does not unduly affect the algorithms.

3.1.1. Noise removal

Having a transparent and unambiguous set of images at hand is essential for creating a dependable image identification method. Therefore, the first step in extracting the important information from the image is to remove the background noise for both traditional image processing and deep learning approaches. Equation (1) shows the general framework of additive noise in the field of digital image processing in which $h(x, y)$ denotes the original pre-filtering image, $f(x, y)$ is the content information, and $n(x, y)$ is the additive white noise.

$$h(x, y) = f(x, y) + n(x, y) \quad (1)$$

Assuming that the noise $n(x, y)$ has a zero-mean distribution, we can extract the content information by taking the expected value of $h(x, y)$ (Yang et al. 2014):

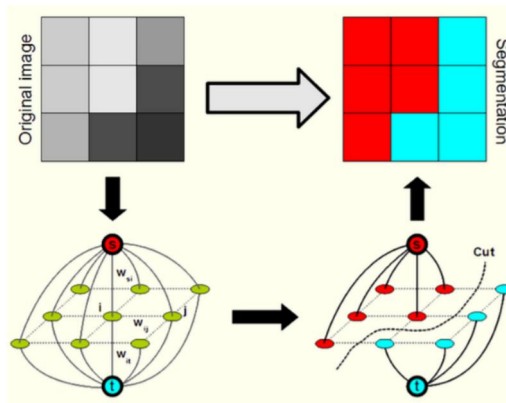


Figure 3. The unsupervised GrabCut algorithm illustration.

$$Eh(x, y) = f(x, y) + En(x, y) = f(x, y) \quad (2)$$

Moreover, with no prior assumption or knowledge about the noise distribution, we can approximate the content of the image by simply averaging over the image pixels. With this method, the random digital noise can be decreased.

3.2. Image segmentation

Image segmentation is a process that consists of separating an image into two or more different regions (Sun et al. 2013). To decrease the amount of image information and graphic complexity, we can conduct image segmentation to detect the staff gauge and water line. Numerous methods for segmenting images have been put forth in the literature; some of these methods are thought to be universal, while others are tailored to particular image classes. The work of Haralick and Shapiro (1985) provides a great survey of the existing methods, though these algorithms require a significant processing time. Image segmentation is an essential step for water line detection. The main assumption in the image segment method for water line detection is that the water level draws a line on the measurement staff gauge (Ren et al. 2007; Shin et al. 2008). In this approach, each column of grayscale image pixels is scanned from top to bottom to find a sharp and noticeable change in the pixel intensity level. However, this approach is only suitable for staff gauge images with a simple background where the water level draws a clear line on the staff gauge (Gilmore et al. 2013). When the image background is composed of more complicated patterns, with some horizontal lines similar to that of the water level, it is difficult to distinguish between the actual water level and other lines in the segmented image. Thus, in this paper, we develop and analyze two methods for image segmentation and eventually select the region of interest. The first method is the GrabCut algorithm, a traditional approach for segmenting the foreground from the background, and the second one is a deep learning approach using Mask-Region-based Convolutional Neural Network (Mask-RCNN) (Figure 3).

3.2.1. Segmentation using GrabCut algorithm

We employ the GrabCut algorithm which is an iterative and minimal user intervention algorithm for unsupervised image segmentation tasks, splitting the images into foreground and background (Rother et al. 2004). In this work, we use GrabCut for the segmentation of the gauge from the rest of the image. The algorithm is usually implemented by using an input image with either a bounding box that specifies the location of the object in the image we want to segment or a mask that approximates the segmentation. We first used a threshold binary image to find the maximum contour and then created a mask. Traditional image segmentation methods employ texture (color) information or edge (contrast) information. GrabCut successfully combines both forms of information and provides enhanced results.

With a k Gaussian component ($k = 5$) full covariance mixed Gaussian mode (GMM), we represent the target and backdrop in RGB color space (GMM). As a result, there is an additional vector, which corresponds to the Gaussian component of

the n_{th} pixel. A Gaussian component of the target GMM or a Gaussian component of the background GMM is used for each pixel. Consider the $z = \{z_i, \dots, z_n, \dots, z_N\}$ of N pixels for a color image I , where $Z_i = R_i + G_i + B_i, I[1, \dots, N]$ in RGB space. The segmentation is represented in an array given as, $\alpha = (\alpha_1, \dots, \alpha_N)$, $\alpha_i \in \{0, 1\}$; this assigns a label to each pixel of the image indicating whether it belongs to the background or foreground. For GMM, an additional vector $k = \{k_i, \dots, k_n, \dots, k_N\}$ is introduced to optimize the network, which represents a single GMM component, one from either the background or foreground model. A trimap T is created consisting of a background (T_B), foreground (T_F), and uncertain pixels (T_U). The GrabCut algorithm won't be able to modify T_B and T_F labels. For background pixels ($\alpha_i = 0$) covariance GMM of k components are defined and for foreground pixels ($\alpha_j = 1$), parameterized as follows:

$$\theta = \{\pi(\alpha, k), \mu(\alpha, k), \sum (\alpha, k), \alpha \in \{0, 1\}, k = 1 \dots k\} \quad (3)$$

Where π is the weights, μ is the means, and Σ the covariance.
So, the Gibbs energy function for segmentation is given as:

$$E(\alpha, k, \theta, z) = U(\alpha, k, \theta, z) + V(\alpha, z) \quad (4)$$

Where U is a regional item that denotes a penalty for classifying a pixel as a target or background. Considering the probability distribution of the model and considering the neighborhood pixel C .

$$U(\alpha, k, \theta, z) = \sum_i i- \log z_i | \alpha_i, k_i, \theta) - \log \pi(\alpha_i, k_i) \quad (5)$$

$$V(\alpha, z) = \gamma \sum \{m, n\} \in C [\alpha n \neq \alpha m] \exp(-\beta ||z_m - z_n||_2) \quad (6)$$

The final segmentation is accomplished using a minimum cut algorithm with this energy minimization scheme and given the starting trimap T (Hernández-Vela et al., 2012). The GrabCut algorithm is summarized below:

Algorithm:

1. Initialization of the Trimap T .
2. Initialize $\alpha_i = 0$ for $i \in T_B$ and $\alpha_i = 1$ for $i \in T_U \cup T_F$
3. Using k -means, create Background and Foreground GMMs from sets $\alpha_i = 0$ and $\alpha_i = 1$ respectively.
4. Assign pixels to GMM components.
5. Use data z to learn GMM parameters.
6. Use graph cuts to estimate segmentation.
7. Continue from step 4 until convergence is achieved.

The algorithm is guaranteed to reach a local minimum of E . It is simple to identify when E stops decreasing significantly and to automatically stop the iteration.

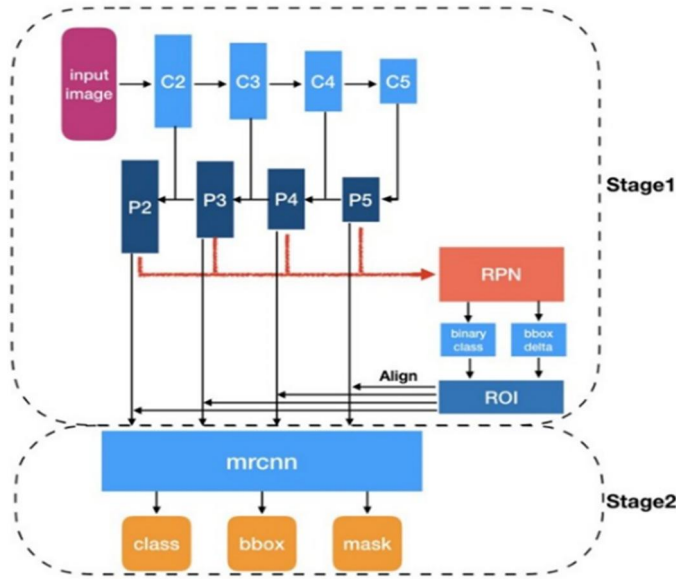


Figure 4. The architecture of the Mask RCNN segmentation algorithm.

3.2.2. Segmentation using Mask-RCNN

As shown in Figure 4, using Mask R-CNN, we can also automatically segment and construct pixel-wise masks for the gauge. The Mask R-CNN algorithm was developed by (He et al. 2017) and builds on the previous works of R-CNN (Girshick et al. 2014), Fast R-CNN (Girshick 2015), and Faster R-CNN (Ren et al. 2015). There are mainly two stages for Mask RCNN. First, it generates proposals regarding where the object might be on the input image. Second, it predicts the class of the object created by the bounding box and generates a pixel-level mask. These two stages are connected to the backbone structure which is a feature pyramid network (FPN) deep neural algorithm consisting of a bottom-up, a top-bottom pathway, and lateral connections. The bottom-up pathway can be any ConvNet, which extracts features from raw images. The top-bottom pathway generates a feature pyramid map. Lateral connections are convolution and adding operations between two corresponding levels of the two pathways accordingly.

The essential missing ingredient of Fast/Faster R-CNN is pixel-to-pixel alignment, which is fulfilled in the Mask R-CNN algorithm. The Mask R-CNN uses the same two-stage technique as Mask R, with the same first stage (RPN). Mask R-CNN outputs a binary mask for each region of interest in the second stage, in addition to predicting the class and box offset. This contrasts with most contemporary systems, which rely on mask predictions for categorization. The Mask R-CNN model is easy to develop and train, thanks to the Faster R-CNN framework, which allows for a variety of configurable architecture designs. Furthermore, the mask branch adds only a modest amount of computational overhead, allowing for rapid computation. It comprises of backbone Network, Region Proposal Network, mask Representation, and RoI Align. The RoI Align layer is used to correct location misalignment in RoI pooling due to quantization. RoI Align reduces hash quantization, for example, by using $x/16$ instead of $[x/16]$, allowing the extracted features to be aligned with the input

pixels properly. The floating-point position values in the input are computed *via* bilinear interpolation. Mask R-multi-task CNN's loss function integrates classification, localization, and segmentation of mask losses, as defined by:

$$L = L_{cls} + L_{box} + L_{mask} \quad (7)$$

Where L_{box} is ignored for background RoI by the indicator function $1[u \geq 1]$, defined as:

$$1[u \geq 1] = \{1 \text{ if } u \geq 1 \text{ } 0 \text{ otherwise} \quad (8)$$

Where L_{mask} is defined as the average binary cross-entropy loss:

$$L_{mask} = -1/m^2 \sum_{1 \leq i, j \leq m} [y_{ij} \log y_{ij}^k + (1 - y_{ij}) \log (1 - y_{ij}^k)] \quad (9)$$

Where (i, j) is the cell and y_{ij} is the label of the cell, and y_{ij}^k is the predicted value of that same cell in class k.

The branch mask creates a mask with dimensions of $m \times m$ for each RoI and each class, totaling k classes. As a result, the entire output is of the size K. There is no competition among classes for producing masks because the model is attempting to learn a mask for each class. We have used the following metrics to evaluate the implemented Mask-RCNN model. The accuracy indicates the correctness of sample predictions whether positive or negative. The precision indicates the proportion of correct water samples to all of the samples predicted as truth and the F1 score takes into account the precision and recall. The confusion matrix, which includes true positives, false positives, true negatives, and false negatives, is used to calculate all of the metrics. The accuracy is the ratio of true positives (TP) with a total number of pixels, as defined by:

$$OA = \frac{TP}{TP + FP + FN + TN} \quad (10)$$

Where, TP = true positives, FP = false positives, FN = false negatives, and TN = true negatives.

Other statistical validation metrics, including Precision, Recall, and F1-score were also calculated, as defined by:

$$Precision = \frac{TP}{TP + FP} \quad (11)$$

$$Recall = \frac{TP}{TP + FN} \quad (12)$$

$$F1 - Score = 2 \times \frac{Precision \times Recall}{Precision + Recall} \quad (13)$$

3.3. Gauge reading

After obtaining the region of interest, the next step is to identify the water line. We analyze and compare two approaches to solving the problem of identifying the water gauge reading. By separating the background and foreground of the image and decreasing the amount of image information and graphic complexity, detecting the water level line will be straightforward and accurate. Here we implement and study two approaches, one is gauge reading using image registration, and the other is gauge reading using pixel calibration.

3.3.1. Water level reading using image registration

In this approach, the water line is detected by identifying the maximum value of gray value difference in the region of the water line. The final actual water level is obtained by using the physical resolution of the template image. In this step, we perform feature matching and align the candidate image to the template image by implementing image registration. Image registration is the process of transforming different images of one scene into the same coordinate system. These different images can be taken from different perspectives, and they can be registered using different methods. The resulting coordinate system can be used to represent different scenes. Image registration is common in the field of medical imagery, as well as satellite image analysis and optical flow. Since the early 2000s, most image registration techniques have mostly relied on feature-based approaches. These methods involve three main steps: key point detection, feature matching, and image warping. Thus, we select points of interest for both the template image and the segmented image and transform them so that the segmented image is aligned with the reference image (i.e. the template image). A key point is defined as a feature or characteristic of an image that is important to people who are interested in it. A descriptor is a feature vector that contains the key points' essential characteristics. In this paper, we use the scale-invariant feature transform (SIFT) feature descriptor. SIFT is a key point detection algorithm that is not free for commercial use, and it is invariant to uniform scaling, orientation, and brightness changes. Then, we need to match the key points between the two images. In this work, we use Fast Library for Approximate Nearest Neighbors (FLANN) for feature matching. FLANN is a fast algorithm that matches images with approximate neighbors in high-dimensional spaces. After picking up the top match, the next step is to find the homography transform and warp the image, this will give us the desired aligned image.

3.3.2. Water level reading using calibrated pixel

In this approach, we use a rather simple and effective method to obtain the water level reading. Here we are measuring the size of the segmented gauge from Mask-RCNN based on the bounding box height. To put it in simple words, we are measuring the size of an object in an image which is similar to computing the distance from the camera to an object – in both circumstances, a ratio that measures the number of pixels per metric must be defined.

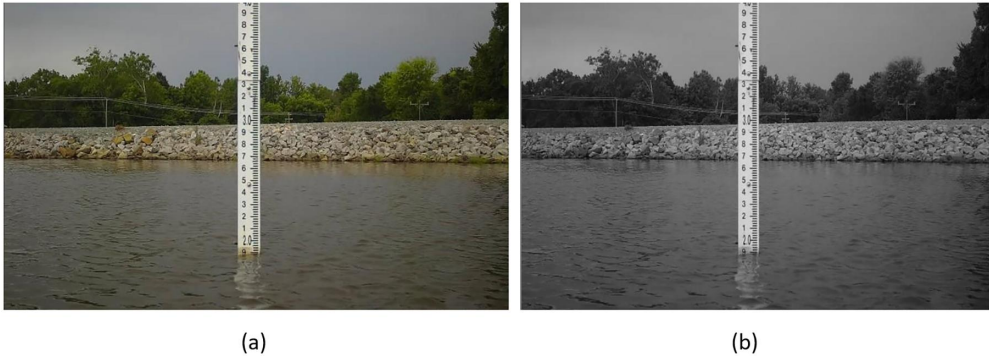


Figure 5. The results of an enhanced image with confidence percentage under low light: (a) original image, (b) noise reduction and grayscale.

4. Results

4.1. Preprocessing

As described in previous subsections, the first step would be image preprocessing to enhance the results of the developed unsupervised and supervised segmentation techniques. [Figure 5\(a\)](#) illustrates the original image of the gauge and [Figure 5\(b\)](#) presents the results of the noise reduction and gray scaling process.

4.2. Image segmentation

In order to reduce the computational cost of image processing, the smallest rectangular area containing the staff gauge above the water surface is cropped and considered as the region of interest (RoI).

4.2.1. Image segmentation results of GrabCut algorithm

To implement the GrabCut algorithm, there are several open-source libraries available, including OpenCV which we used in this paper. In particular, as the ambient light decreases in the late afternoon, extracting the gauge information becomes exceedingly challenging. As explained in previous sections, it is necessary to have a reliable image identification technique. As shown in [Figure 6](#), the required information using the GrabCut algorithm from the preprocessed image has been extracted. The GrabCut algorithm was implemented using Python 3.7 language and OpenCV computer vision library. We observed that the GrabCut algorithm works perfectly on images taken in daylight and lowlight conditions. It is a simple process to obtain the region of interest. However certain problems were encountered during our experiments. The algorithm fails to detect the region of interest on nighttime data; thus, it is not possible to detect the water line and is eventually unable to get the gauge reading during nighttime using an RGB camera. Online monitoring of large water bodies, such as lakes and rivers is crucial during flooding at nighttime using RGB cameras. Also, the ruler has repetitive number divisions, due to this the matching can pick up the wrong features and the image alignment might not be perfect. This can sometimes result in errors in the water line reading. So, to overcome these errors, we used

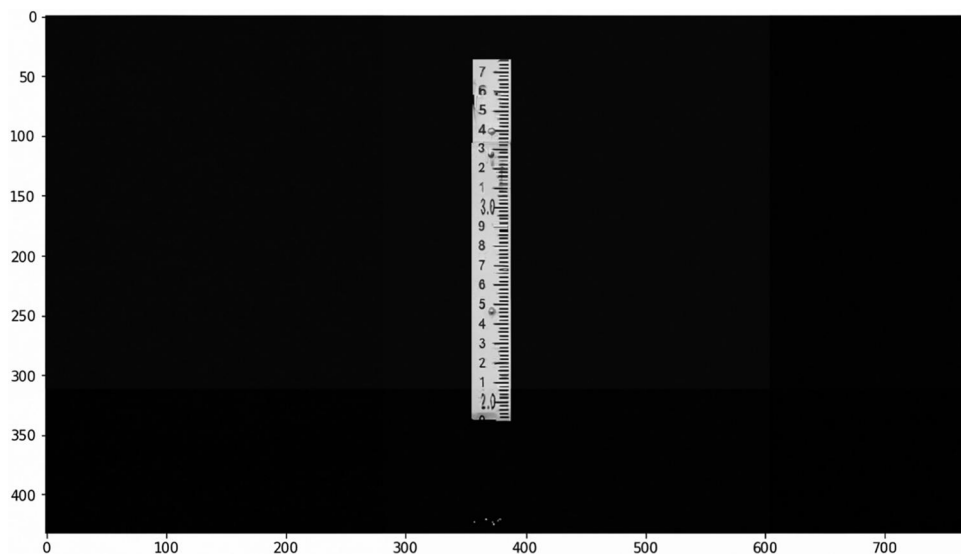


Figure 6. The results of the unsupervised GrabCut algorithm.

another approach using deep learning to segment the gauge region in the next section. Also, failures can occur in the case of (i) regions of low contrast at the transition from foreground to background, and (ii) camouflage, in which the true foreground and background distributions overlap partially in color space.

4.2.2. Image segmentation results of the Mask-RCNN

First, the image dataset was collected and annotated. We collected images under different daylight conditions such as rainy days, low light in the evening, and foggy days. We used 150 images, 100 for training, 30 for testing, and 20 for validation. The deep learning model was trained by only 20 epochs on a Tesla P100 GPU. The next step was to train the Mask RCNN segmentation algorithm on the developed dataset. In the final stage, we tested the capability of the developed deep learning model on the test dataset to detect the bounding boxes, classes, and confidence percentages. The segmentation results are shown in Figures 7 and 8. The obtained results illustrated that compared to the unsupervised segmentation model of GrabCut, the Mask-RCNN resulted in better segmentation performance. Figure 7 presents the segmentation results of the Mask-RCNN with the confidence percentage under low light conditions and Figure 8 shows the results of the segmentation during nighttime. The batch size was set to 8 and the learning rate to 0.001 with a Momentum of 0.9. The model performed well with the weight decay of $5e-4$. The other hyperparameters in training were SGD + momentum (Optimizer), MultiStepLR (Scheduler), ResNet50 + FPN (Backbone), and Gamma of 0.1. The training accuracy, validation loss, and training loss are illustrated in Figure 9. As shown in Table 1, the deep learning model of the Mask RCNN resulted in an accuracy, precision, and F-1 score of 0.86, 0.97, and 0.93, respectively. As the results indicate, the developed deep learning method provided reliable measurement even in low ambient light environments as well as nighttime compared to the GrabCut algorithm which failed to provide satisfactory segmentation results under low light and nighttime conditions.

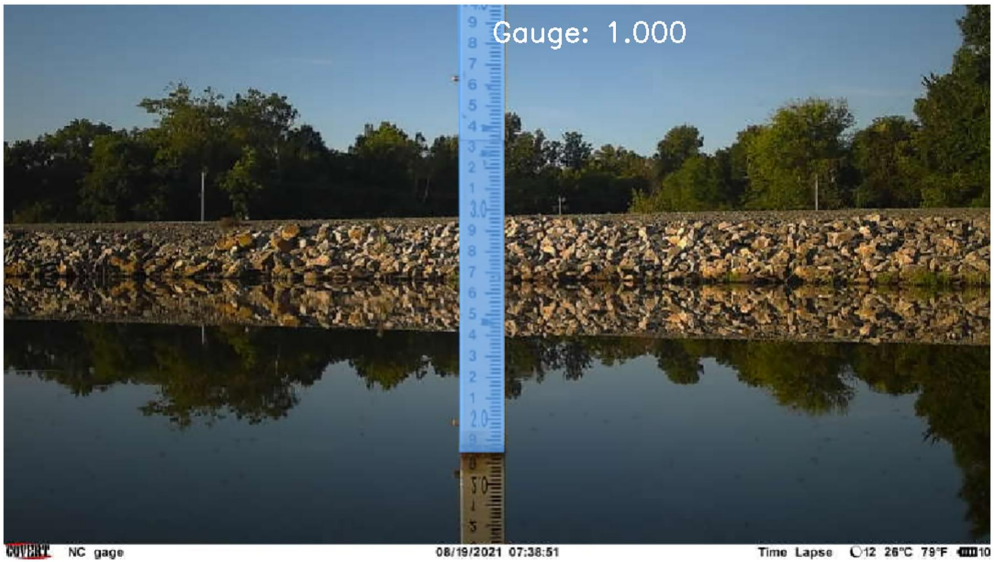


Figure 7. The results of the mask RCNN segmentation model with confidence percentage under low light conditions.

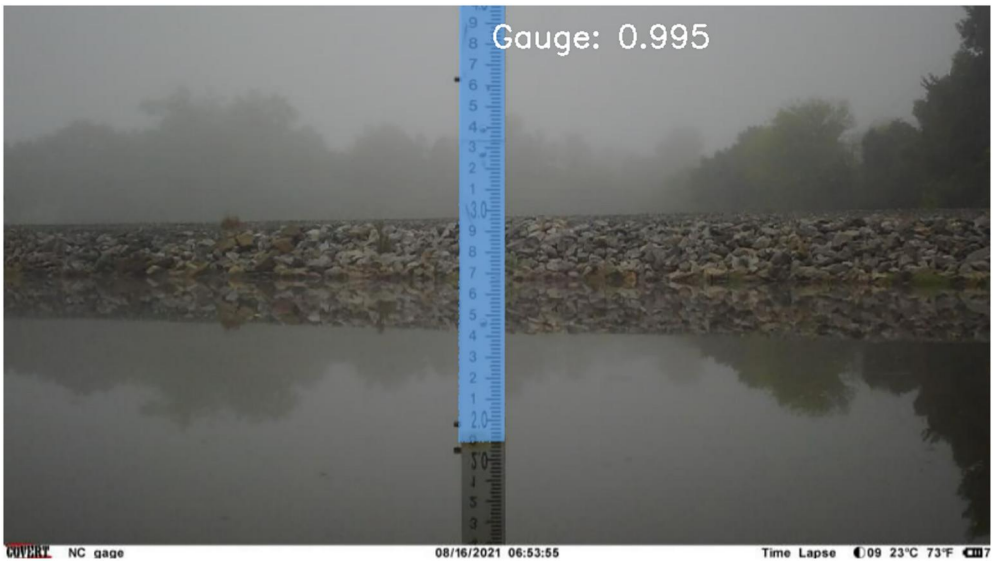


Figure 8. The results of the mask RCNN segmentation model with confidence percentage during evening time.

4.3. Results of the gauge reading methods

Considering the issue of clear visibility under low light and nighttime, as discussed there are two different gauge reading methods. The results of the gauge reading are discussed below.

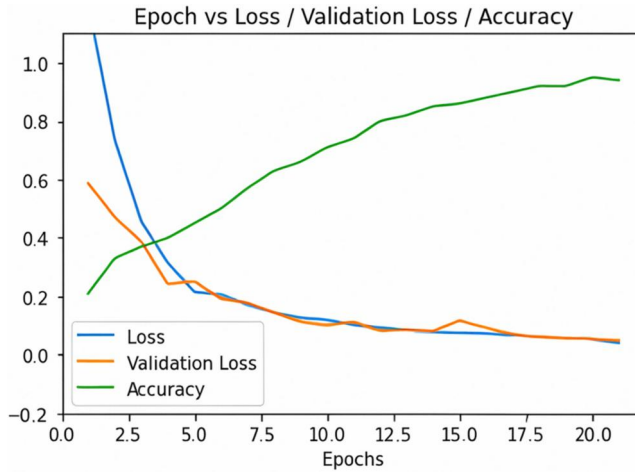


Figure 9. The accuracy, training loss, and validation loss curves of the mask-RCNN segmentation model.

Table 1. The confusion matrix of the Mask-RCNN segmentation model.

Actual values	Predictive values	
	Positive (1)	Negative (0)
Positive (1)	TP = 130	FN = 15
Negative (0)	FP = 3	TN = 2

4.3.1. Results of the water level reading using image registration method

The horizontal projection method is the most widely used method (Zhang et al. 2019) for standard bi-color water gauges. The water line position can be determined by searching and finding the points where the abrupt change points occur, and reading can be obtained by summing up all the gray pixel values in the X-direction and creating the horizontal projection curve. Based on the style of the standard gauge, a binary orthographic template image is designed as shown in Figure 10(a). As we can observe in Figure 10(e), there is a sudden change in the region between the gauge and the water surface. This projection figures in the pixel value and location of the waterline. Thus, the waterline is converted to an actual waterline reading with the physical resolution of the template image. For example, in the registered image in Figure 10(d), we see the reading is near 400 pixels along the Y-axis. The reading starts from the bottom level, so we must change the value from 400 to Ruler Height – 400. To get the correct reading, we have to multiply it with the calibrated pixel value which can be obtained by dividing the actual length of the ruler by the template image's height. For example, for the shown image, the correct gauge reading can be calculated as:

$$(900 - 400) * 0.0036 \sim 1.84 \quad (14)$$

The discussed method provided good results and successfully calculated the gauge reading. However, one major drawback of this approach was that, for template matching, we require features to match and align, and these features are the gauge

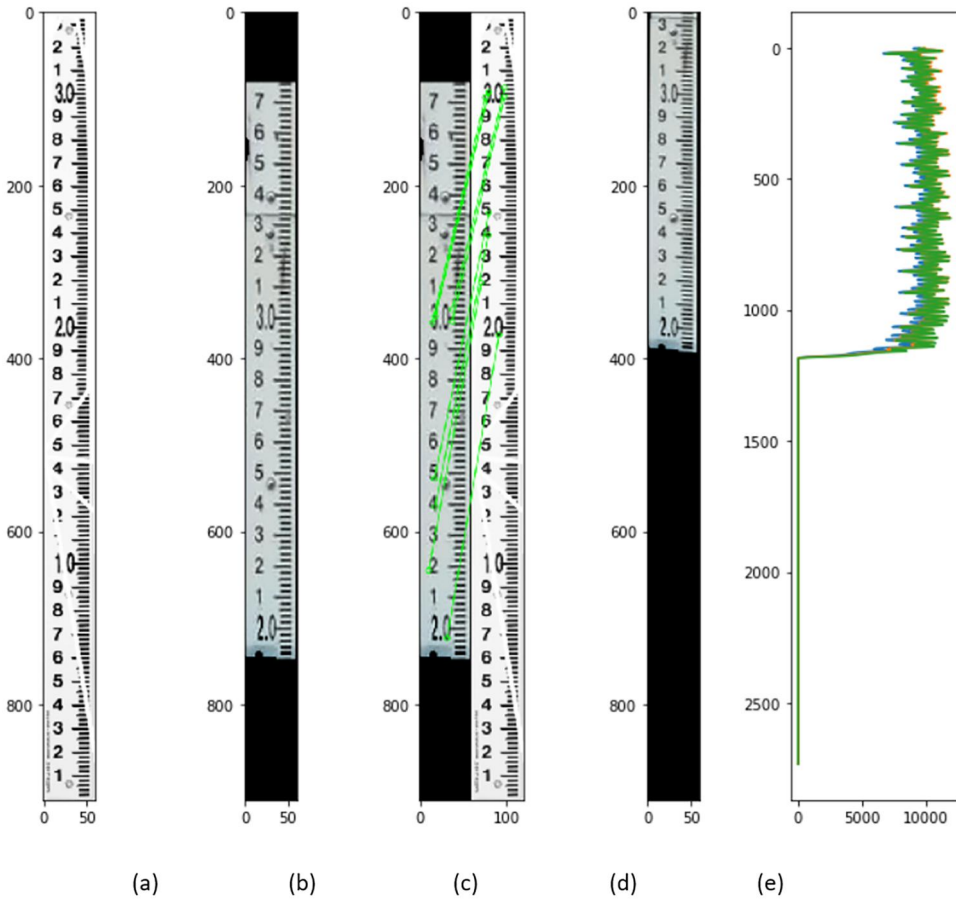


Figure 10. Examples of (a) template, (b) segmented image, (c) template matching, (d) image alignment, and (e) water level reading.

line markings and numbers. During the night, the flash of the camera is completely reflected from the gauge and the numbers are not visible. Thus, it would be impossible to use this method during nighttime due to the fact that the numbers and lines are not visible, as seen in Figure 11. The results indicated that while the mask-RCNN could segment the region of interest successfully during nighttime, with the image registration technique, it was impossible to get the correct water level reading.

4.3.2. Results of the water level reading using calibrated pixel method

In our measurement site, the camera is firmly fixed at a certain location and so is the gauge. Given the fact that the location of the camera and the gauge do not change, we can obtain the water level. Since we already have an understanding of the scale distribution of the gauge, it is easy to understand the relation between the scale units and pixel distribution. We already found this relation and calculated the calibrated pixel value in the previous section, we can directly use that to our benefit here. We can use the same calibrated pixel value at nighttime because the locations of our camera and the gauge remain constant. So, we use this pixel value to multiply with the height of the bounding

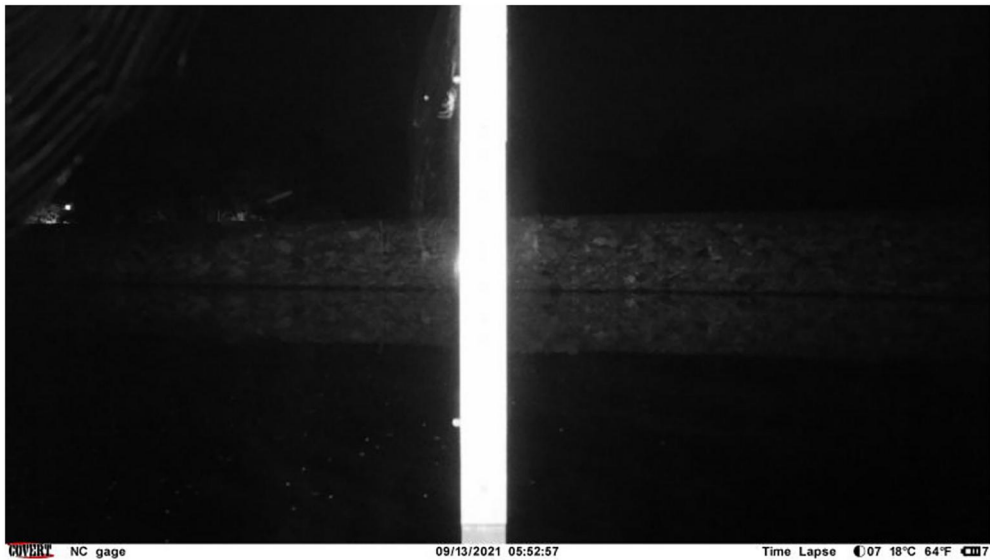


Figure 11. An example of an image taken during nighttime.

box from mask-RCNN output to obtain the gauge reading. Thus, we can successfully get our gauge reading even at nighttime even though the ruler markings are not visible.

4. Discussion

Given that floods are one of the most expensive and destructive natural disasters, there is an immense demand for an IoT system for flood monitoring and forecasting. Early warning of impending flooding can be provided by an IoT system, allowing citizens and rescue personnel to take the appropriate safety measures to safeguard themselves and their property. This can lessen the effects of floods on society, the economy, and lives lost. In the context, water gauge readings are essential for providing ground truth measurements of water levels in rivers, lakes, and reservoirs as well as initializing, calibrating, and validating weather models and providing early warning and insights into hydrological responses to weather events (Ming et al. 2020).

In addition to providing early warnings, the low-cost IoT system can also help improve our understanding of the factors contributing to flooding. By collecting and analyzing large amounts of data from sensors in real-time, the system can identify patterns and trends that may not be immediately apparent. This can help us better understand the causes of floods and develop more effective strategies for mitigating their impacts. An IoT system can also be integrated with other technologies to provide a more comprehensive view of the situation, enabling more effective flood management efforts. many real times flood monitoring and prediction systems used by first responders such as FIMAN (the Flood Inundation Mapping and Alert Network) integrates water gauge data and Digital Elevation Models (DEMs) to identify inundated areas (<https://fiman.nc.gov/>). Low-cost IoT solutions offer several advantages and limitations. The systems are relatively easy to deploy, affordable, and capable of covering large areas through distributed cameras and sensors. Their accessibility and

potential for remote monitoring make them a promising alternative to traditional systems (Zikria et al. 2019; Rani et al. 2020). Continuous gauge readings through the IoT solution enables providing real-time data that can dynamically update weather models or inundation maps, ensuring an accurate flood monitoring system, especially when conditions change with recent advancements in cloud computing, data from IoT systems can be quickly integrated with other data through cloud services, enabling accurate and advanced data analytics and near real-time decision-making for effective flood response and management. However, despite the advantages, there are limitations and challenges to consider. The IoT systems generally rely on stable internet connections, which can be challenging during flooding events, especially in remote regions. Other considerations include the quality of sensors, system power management, and compliance with data privacy regulations, all of which are critical for data accuracy and robustness. Despite these considerations and limitations, the increased accessibility and (near) real-time flood monitoring capabilities of low-cost IoT solutions make them a promising option, particularly in flood-prone areas and remote regions. In this research, solar panels are used as a reliable power source to mitigate the issue of frequent battery replacements. Additionally, the data collected is managed according to state agency regulations and entered into Contrail for inclusion in NC FIMAN. This research also leverages a low-cost IoT system to enhance real-time data collection (images) and developing deep learning models to quickly analyze and extract water levels from the large gauge dataset, which will improve flood prediction models and their integration into broader flood monitoring networks which was proved in the paper.

The proposed IoT-based water level measurement method in the research can effectively monitor the water level in large water bodies, such as rivers and lakes. The motivation behind employing image-based methods for monitoring the water level stems from the recent advancements in IoT systems. In particular, the on-site cameras are connected to cloud centers where they can directly upload the images without a limitation on their memory capacity. Furthermore, thanks to the proliferation of advanced cloud computing capabilities, the proposed method can run in real-time for online monitoring of the water reservoirs. As the proposed method is completely autonomous and does not require any human interaction in the loop or expert knowledge, several practical applications are envisioned. First, when the likelihood of flood is increased beyond a certain point, the fully autonomous system can dispatch a signal to the corresponding responsible units for deploying disaster management/relief protocols. Second, constant and real-time monitoring of the water reservoirs can potentially help to build comprehensive knowledge about sudden and abrupt climate events and improve our ability to predict such events in advance and design suitable safety protocols. Finally, monitoring and measuring the level of water with IoT-based systems will protect users from running into serious problems, such as water outages in the areas where daily supplies of water are obtained from the neighboring water bodies.

We implemented and compared the results of two methods for segmenting the gauge region from the background. The first one was the unsupervised segmentation model of GrabCut which is a traditional image processing approach. The second method was the mask-RCNN as a deep learning supervised segmentation technique.

The results demonstrated that the GrabCut algorithm provided satisfactory segmentation results only under circumstances where the marking on the ruler was clearly visible. On the other hand, the deep learning algorithm of the Mask-RCNN overcame this issue by successfully classifying the region of interest both under daylight and at nighttime conditions. In the next step to detect the reading of the gauge, we used the image registration technique as a well-known and proven approach. However, results illustrated that the algorithm proved to be only working under daytime or conditions where the ruler markings were visible, which is not feasible during nighttime. So given the fact that the camera and gauge location remain stable, we used a successful method to obtain the gauge reading regardless of the light exposure, which is pixel calibration. To conclude, by trying and testing different methods, we have successfully developed a low-cost IoT-based method to autonomously read the water gauge measurement for flood monitoring which is not affected by poor visibility and illumination conditions.

Apart from the potential benefits of the proposed methodology, one needs to also consider its limitations. Although this method works well in almost all adverse illumination conditions, including nighttime and rainfall, it cannot be applied in dense and heavy fog at night, due to the low visibility of the gauge itself and glare from the camera lights. We developed and analyzed the best possible approach for the gauge reading given that the location of the camera and the gauge remains constant. There exist some technical difficulties that are mainly associated with the RGB images. One possible extension to the current research, which is the problem of having different image scales, is to consider reading the gauge numbers by taking advantage of RADAR images and using deep learning models along with it. As a final note on the implementation of the proposed algorithm, it is worth noting that image identification and analysis might be performed through various platforms. For this project, we used Python 3.7 to implement the proposed algorithms. One particular reason that makes Python our preferred choice of implementation is its effectiveness and capability to work with image data.

5. Conclusion

A real-time water level image obtained during a flood is an efficacious and valuable source of information. In this research, we developed and evaluated several image processing methods for automatic water level measurement which is a critical step for providing timely, detailed, and accurate flood inundation information to local community officials and the public to reduce the loss of life and flood-related property damage. This research proposed a cost-effective and practical methodology for real-time water level measurement while considering the real-world scenarios where the on-site camera is displaced, or the ambient light is not enough for obtaining a high-quality image. Two techniques for distinguishing the gauge region from the surrounding area were put into practice, and the outcomes were assessed. The first was GrabCut's unsupervised segmentation approach, while the second adopted approach was a supervised deep learning segmentation technique called mask-RCNN. The outcomes showed that the GrabCut algorithm could only produce good segmentation outcomes in situations where the ruler's marking was clearly visible. However, this problem was resolved by

Mask-RCNN's deep learning approach, which was able to classify the region of interest both during the day and at night. Therefore, the findings of this study suggest that applying image recording and identification for measuring water levels is an effective approach for extracting necessary information during the flood. This information can be used to launch a timely and well-thought-out operation to prevent or at least minimize the potential damage due to flash floods. In particular, the goal of this study was to provide the observers and decision-makers with valuable information about the intensity and the depth of the flooded areas which can be used for flood prevention engineering design for disaster management protocols. The main contribution of this study was to develop a low-cost and real-time method for acquiring the water level. In this research, the image identification process entailed image processing principles, such as noise filtering, grayscale transformation, image segmentation, and template matching. The developed algorithms are especially suitable for IoT-based online water level monitoring where the on-site images captured by the camera can be efficiently processed using cloud-based computation toolkits and systems. The simulation results prove that the proposed methodology provides reliable measurement even at nighttime or when the original image is distorted due to undesired movements of the camera, which is a common scenario during intense wind and flood.

Disclosure statement

No potential conflict of interest was reported by the author(s).

Funding

This work was supported in part by NC Collaboratory's Accuracy Assessment for IoT Stream Gages Data project, NOAA award NA21OAR4590358, and NASA award 80NSSC23M0051. The testbed and the IoT system for the project were developed by the North Carolina Geodetic Survey team at the NC A&T State Farm.

Data availability statement

The data used in this study is confidential.

References

- Akbar YM, Musafa A, Riyanto I. 2017. Image processing-based flood detection for online flood early warning system. <https://osf.io/preprints/inarxiv/ayn2c>.
- Allamano P, Claps P, Laio F. 2009. Global warming increases flood risk in mountainous areas. *Geophys Res Lett*. 36(24). doi: [10.1029/2009GL041395](https://doi.org/10.1029/2009GL041395).
- Annis A, Nardi F. 2019. Integrating VGI and 2D hydraulic models into a data assimilation framework for real time flood forecasting and mapping. *Geo-Spatial Inform Sci*. 22(4): 223–236. doi: [10.1080/10095020.2019.1626135](https://doi.org/10.1080/10095020.2019.1626135).
- Baek S, Kim KI, Kim TK. 2020. Weakly-supervised domain adaptation via gan and mesh model for estimating 3d hand poses interacting objects. *Proceedings of the IEEE/CVF Conference on Computer Vision and Pattern Recognition*. p. 6121–6131.

- Basnyat B, Roy N, Gangopadhyay A. 2018. A flash flood categorization system using scenetext recognition. 2018 IEEE International Conference on Smart Computing (SMART COMP). IEEE. p. 147–154.
- Fukami K, Yamaguchi T, Imamura H, Tashiro Y. 2008. Current status of river discharge observation using non-contact current meter for operational use in Japan. World Environ Water Resour Congress 2008 AHUPUA'A. :1–10. doi: [10.1061/40976\(316\)278](https://doi.org/10.1061/40976(316)278).
- Gebrehiwot A, Hashemi-Beni L, Thompson G, Kordjamshidi P, Langan TE. 2019. Deep convolutional neural network for flood extent mapping using unmanned aerial vehicles data. *Sensors*. 19(7):1486. doi: [10.3390/s19071486](https://doi.org/10.3390/s19071486).
- Gebrehiwot A, Hashemi-Beni L. 2020. Automated inundation mapping: comparison of methods. In IGARSS 2020–2020 IEEE International Geoscience and Remote Sensing Symposium; Waikoloa, HI, USA: IEEE; p. 3265–3268.
- Gebrehiwot A, Hashemi-Beni L. 2020. A method to generate flood maps in 3D using DEM and deep learning. *The international archives of photogrammetry. Remote Sens Spat Inform Sci*. 44:25–28.
- Gebrehiwot Asmamaw, Hashemi-Beni Leila, Thompson Gary, Kordjamshidi Parisa. 2019. Deep convolutional neural network for flood extent mapping using unmanned aerial vehicles data. *Sensors*. 19(7):1486.
- Gilmore TE, Birgand F, Chapman KW. 2013. Source and magnitude of error in an inexpensive image-based water level measurement system. *J Hydrol*. 496:178–186. doi: [10.1016/j.jhydrol.2013.05.011](https://doi.org/10.1016/j.jhydrol.2013.05.011).
- Girshick R. 2015. Fast r-Cnn. In *Proceedings of the IEEE International Conference on Computer Vision*. Santiago, Chile: IEEE; p. 1440–1448.
- Girshick R, Donahue J, Darrell T, Malik J. 2014. Rich feature hierarchies for accurate object detection and semantic segmentation. In *Proceedings of the IEEE Conference on Computer Vision and Pattern Recognition*. Columbus, OH, USA: IEEE. p. 580–587.
- Han Z, Lv N, Ai X, Zhou Y, Jiang J, Chen C. 2022. Water gauge image augmentation based on generative adversarial network. In 2022 IEEE International Conference on Smart Internet of Things (SmartIoT). IEEE. p. 154–160.
- Haralick RM, Shapiro LG. 1985. Image segmentation techniques. *Comput Vis Graph Image Process* 499. 29(1):100–132. doi: [10.1016/S0734-189X\(85\)90153-7](https://doi.org/10.1016/S0734-189X(85)90153-7).
- Hashemi-Beni L, Gebrehiwot AA. 2021. Flood extent mapping: an integrated method using deep learning and region growing using UAV optical data. *IEEE J Sel Top Appl Earth Observ Remote Sens*. 14:2127–2135. doi: [10.1109/JSTARS.2021.3051873](https://doi.org/10.1109/JSTARS.2021.3051873).
- He K, Gkioxari G, Dollár P, Girshick R. 2017. Mask r-Cnn. *Proceedings of the IEEE International Conference on Computer Vision*. Venice, Italy: IEEE.
- Hernández-Vela A, Reyes M, Ponce V, Escalera S. 2012. Grabcut-based human segmentation in video sequences. *Sensors*. 12(11):15376–15393. doi: [10.3390/s121115376](https://doi.org/10.3390/s121115376).
- Husni M, Siahaan DO, Ciptaningtyas HT, Studiawan H, Amp, Aliarham YP. 2016, April. Liquid volume monitoring based on ultrasonic sensor and Arduino microcontroller. Vol. 128, No. 1. IOP Conference Series: Materials Science and Engineering. IOP Publishing. p. 012026.
- Jafari NH, Li X, Chen Q, Le CY, Betzer LP, Liang Y. 2020. Real-time water level monitoring using live cameras and computer vision techniques. *Comput Geosci*. 147:104642. doi: [10.1016/j.cageo.2020.104642](https://doi.org/10.1016/j.cageo.2020.104642).
- Li Y, Martinis S, Wieland M. 2019. Urban flood mapping with an active self-learning convolutional neural network based on TerraSAR-X intensity and interferometric coherence. *ISP RS J Photogramm Remote Sens*. 152:178–191. doi: [10.1016/j.isprsjprs.2019.04.014](https://doi.org/10.1016/j.isprsjprs.2019.04.014).
- Ling J, Zhang H, Lin Y. 2021. Improving urban land cover classification in cloud-prone areas with polarimetric SAR images. *Remote Sens*. 13(22):4708. doi: [10.3390/rs13224708](https://doi.org/10.3390/rs13224708).
- Ming X, Liang Q, Xia X, Li D, Fowler HJ. 2020. Real-time flood forecasting based on a high-performance 2-D hydrodynamic model and numerical weather predictions. *Water Resour Res*. 56(7):e2019WR025583. doi: [10.1029/2019WR025583](https://doi.org/10.1029/2019WR025583).

- Pan J, Yin Y, Xiong J, Luo W, Gui G, Sari H. 2018. Deep learning-based unmanned surveillance systems for observing water levels. *IEEE Access*. 6:73561–73571. doi: [10.1109/ACCESS.2018.2883702](https://doi.org/10.1109/ACCESS.2018.2883702).
- Rahayu R, Mathias SA, Reaney S, Vesuviano G, Suwarman R, Ramdhan AM. 2023. Impact of land cover, rainfall and topography on flood risk in West Java. *Nat Hazards*. 116(2): 1735–1758. doi: [10.1007/s11069-022-05737-6](https://doi.org/10.1007/s11069-022-05737-6).
- Rani DS, Jayalakshmi GN, Baligar VP. 2020, March. Low cost IoT based flood monitoring system using machine learning and neural networks: flood alerting and rainfall prediction. In 2020 2nd International Conference on Innovative Mechanisms for Industry Applications (ICIMIA); Bangalore, India: IEEE. p. 261–267.
- Ren MW, Yang WK, Wang H. 2007. New algorithm of automatic water level measurement based on image processing. *Jisuanji Gongcheng yu Yingyong [Comput Eng Appl]*. 42:204–206.
- Ren S, He K, Girshick R, Sun J. 2015. Faster R-CNN: towards real-time object detection with region proposal networks. *Adv Neur Inform Process Syst*. :28.
- Rother C, Kolmogorov V, Blake A. 2004. "GrabCut" interactive foreground extraction using iterated graph cuts. *ACM Trans Graph*. 23(3):309–314. doi: [10.1145/1015706.1015720](https://doi.org/10.1145/1015706.1015720).
- Salem A, Hashemi-Beni L. 2022. Inundated vegetation mapping using SAR data: a comparison of polarization configurations of UAVSAR l-band and sentinel c-band. *Remote Sens*. 14(24): 6374. doi: [10.3390/rs14246374](https://doi.org/10.3390/rs14246374).
- Shin I, Kim J, Lee SG. 2008. Development of an internet-based water-level monitoring and measuring system using CCD camera. *ICMIT 2007: Mechatronics, MEMS, and Smart Materials; International Society for Optics and Photonics*. Gifu, Japan: SPIE. Vol. 6794, p. 67944Q.
- Simpson MR. 2001. Discharge measurements using a broad-band acoustic Doppler current profiler. US Department of the Interior, US Geological Survey Reston.
- Smith AB, Katz RW. 2013. US billion-dollar weather and climate disasters: data sources, trends, accuracy and biases. *Nat Hazards*. 67(2):387–410. doi: [10.1007/s11069-013-0566-5](https://doi.org/10.1007/s11069-013-0566-5).
- Sood SK, Sandhu R, Singla K, Chang V. 2018. IoT, big data and HPC based smart flood management framework. *Sustain Comput Informat Syst*. 20:102–117. doi: [10.1016/j.suscom.2017.12.001](https://doi.org/10.1016/j.suscom.2017.12.001).
- Suh S, Park Y, Ko K, Yang S, Ahn J, Shin JK, Kim S. 2021. Weighted mask R-CNN for improving adjacent boundary segmentation. *J Sensors*. 2021(1):1–8. doi: [10.1155/2021/8872947](https://doi.org/10.1155/2021/8872947).
- Sun T, Zhang C, Li L, Tian H, Qian B, Wang J. 2013. Research on image segmentation and extraction algorithm for bicolor water level gauge. 2013 25th Chinese Control and Decision Conference (CCDC). Guiyang, China: IEEE. p. 2779–2783.
- Thai-Nghe N, Thanh-Hai N, Amp, Chi Ngon N. 2020. Deep learning approach for forecasting water quality in IoT systems. *Int J Adv Comput Sci Appl*. 11(8):686–693.
- Villarini G. 2016. On the seasonality of flooding across the continental United States. *Adv Water Resour*. 87:80–91. doi: [10.1016/j.advwatres.2015.11.009](https://doi.org/10.1016/j.advwatres.2015.11.009).
- Xu X, Zhang T, Liu H, Guo W, Zhang Z. 2024. An Information-expanding network for water body extraction based on U-net. *IEEE Geosci Remote Sensing Lett*. 21:1–5. doi: [10.1109/LGRS.2024.3371485](https://doi.org/10.1109/LGRS.2024.3371485).
- Yang HC, Wang CY, Yang JX. 2014. Applying image recording and identification for measuring water stages to prevent flood hazards. *Nat Hazards*. 74(2):737–754. doi: [10.1007/s11069-014-1208-2](https://doi.org/10.1007/s11069-014-1208-2).
- Zikria YB, Kim SW, Hahm O, Afzal MK, Aalsalem MY. 2019. Internet of things (IoT) operating systems management: opportunities, challenges, and solution. *Sensors*. 19(8):1793. doi: [10.3390/s19081793](https://doi.org/10.3390/s19081793).
- Zhang, Z., Zhou, Y., Liu, H., Zhang, L., & Wang, H. (2019). Visual measurement of water level under complex illumination conditions. *Sensors*. 19(19), 4141. doi: [10.3390/s19194141](https://doi.org/10.3390/s19194141).